Theoretical Population Biology xx (xxxx) xxx–xxx

Contents lists available at ScienceDirect

Theoretical Population Biology

journal homepage: www.elsevier.com/locate/tpb

Ecocultural range-expansion scenarios for the replacement or assimilation of Neanderthals by modern humans

Joe Yuichiro Wakano [a,1], William Gilpin [b,1], Seiji Kadowaki [c], Marcus W. Feldman [d,*], Kenichi Aoki [e]

[a] School of Interdisciplinary Mathematical Sciences, Meiji University, Nakano 4-21-1, Nakano-ku, Tokyo 164-8525, Japan
[b] Department of Applied Physics, Stanford University, Stanford CA 94305-5020, USA
[c] Nagoya University Museum, Nagoya University, Furocho, Chikusa-ku, Nagoya 464-8601, Japan
[d] Department of Biology, Stanford University, Stanford CA 94305-5020, USA
[e] Organization for the Strategic Coordination of Research and Intellectual Properties, Meiji University, Nakano 4-21-1, Nakano-ku, Tokyo 164-8525, Japan

ARTICLE INFO

Article history:
Received 1 September 2017
Available online xxxx

Keywords:
Competition
Spatial diffusion
Traveling waves
Multiple wave fronts
Local coexistence conditions
Bladelets/microliths

ABSTRACT

Recent archaeological records no longer support a simple dichotomous characterization of the cultures/behaviors of Neanderthals and modern humans, but indicate much cultural/behavioral variability over time and space. Thus, in modeling the replacement or assimilation of Neanderthals by modern humans, it is of interest to consider cultural dynamics and its relation to demographic change. The ecocultural framework for the competition between hominid species allows their carrying capacities to depend on some measure of the levels of culture they possess. In the present study both population densities and the densities of skilled individuals in Neanderthals and modern humans are spatially distributed and subject to change by spatial diffusion, ecological competition, and cultural transmission within each species. We analyze the resulting range expansions in terms of the demographic, ecological and cultural parameters that determine how the carrying capacities relate to the local densities of skilled individuals in each species. Of special interest is the case of cognitive and intrinsic-demographic equivalence of the two species. The range expansion dynamics may consist of multiple wave fronts of different speeds, each of which originates from a traveling wave solution. Properties of these traveling wave solutions are mathematically derived. Depending on the parameters, these traveling waves can result in replacement of Neanderthals by modern humans, or assimilation of the former by the latter. In both the replacement and assimilation scenarios, the first wave of intrusive modern humans is characterized by a low population density and a low density of skilled individuals, with implications for archaeological visibility. The first invasion is due to weak interspecific competition. A second wave of invasion may be induced by cultural differences between moderns and Neanderthals. Spatially and temporally extended coexistence of the two species, which would have facilitated the transfer of genes from Neanderthal into modern humans and vice versa, is observed in the traveling waves, except when niche overlap between the two species is extremely high. Archaeological findings on the spatial and temporal distributions of the Initial Upper Palaeolithic and the Early Upper Palaeolithic and of the coexistence of Neanderthals and modern humans are discussed.

1. Introduction

Recent archaeological and anthropological findings and analyses suggest that modern humans had reoccupied the Middle East by 55 kya (Hershkovitz et al., 2015) and indicate that they subsequently overlapped with Neanderthals in Europe between about 45 and 40 kya, after which the latter disappeared from Europe (Mellars, 2006a; Benazzi et al., 2011, 2015; Higham et al., 2014; Hublin, 2015; Roebroeks and Soressi, 2016). Although Neanderthal effective population size shows an overall decreasing trend after about 0.5 to 1.0 Mya (Prüfer et al., 2014), the Neanderthal population in Europe during the Middle Palaeolithic may have fluctuated in response to climatic cycles (Hublin and Roebroeks, 2009). Importantly, Neanderthal population appears to have repeatedly recovered when environmental conditions improved and, in particular, may have attained its maximum size, at least in Germany, just before the arrival of modern humans (Richter, 2016). Hence, Neanderthal extinction cannot readily be explained by climate

* Corresponding author.
E-mail address: mfeldman@stanford.edu (M.W. Feldman).
[1] These authors contributed equally.

https://doi.org/10.1016/j.tpb.2017.09.004
0040-5809/

change per se, and given that the two species overlapped and likely exploited similar niches (Banks et al., 2008; Hoffecker, 2009; Nigst et al., 2014; Roebroeks and Soressi, 2016), the most plausible cause of the replacement of the indigenous Neanderthals by the intrusive modern humans is interspecific competition.

What competitive advantage did the modern humans have over the Neanderthals (and other archaic human species in Eurasia)? The prevailing view among archaeologists is that modern humans were culturally/technologically more advanced than the coeval Neanderthals, perhaps because they possessed more advanced cognitive abilities (e.g., Mellars, 2006a, b, c; Klein, 2008; Bar-Yosef, 2013; Wynn et al., 2016). However, this interpretation has been contested by Zilhão et al. (2010), Villa and Roebroeks (2014), and Roebroeks and Soressi (2016) who do not see "*substantial* cognitive and technological differences" [italics added] in the archaeological record. These latter authors favor a strictly demographic scenario, whereby the resident Neanderthals were overwhelmed by the numerically superior modern humans. Genetic and archaeological studies do, on balance, suggest that modern humans were more numerous than the Neanderthals (Atkinson et al., 2009; Prüfer et al., 2014; Mellars and French, 2011; Villa and Roebroeks, 2014; Kuhlwilm et al., 2016), but do not provide a compelling explanation for the numerical disparity.

Dependence of the culture/technology level of a human population on its size – a larger population is predicted to have a higher "culture level" – has been the focus of many theoretical (Shennan, 2001; Henrich, 2004; Strimling et al., 2009; Mesoudi, 2011; Lehmann et al., 2011; Aoki et al., 2011; Kobayashi and Aoki, 2012; Fogarty et al., 2015, in press), psychological (Caldwell and Millen, 2010; Derex et al., 2013; Muthukrishna et al., 2014), archaeological (Clark, 2011; Klein and Steele, 2013), and ethnological (Collard et al., 2016; Read, 2006; Kline and Boyd, 2010) studies. These studies treat population size as a *parameter*, determined by undefined causes or manipulated by the experimenter. But culture level may have a reciprocal effect on population size, in which case the latter should also be assumed to be a variable. Moreover, "[a]ny process of population replacement and extinction reduces ultimately to a question of numbers" (Mellars and French, 2011).

Mathematical models of the coupled dynamics of the size and culture level of a population, where both quantities are variables, are therefore more relevant (Lee, 1986; Ghirlanda and Enquist, 2007; Richerson et al., 2009; Aoki, 2015). They show that the population (in isolation) may exist in either of two states: large with a high culture level, or small with a low culture level. Historical contingency may then determine which of these equilibria is reached. Importantly, the empirical observation that population size and number of tool types are not correlated in ethnographic hunter–gatherers (Collard et al., 2016) does not invalidate these models – the sampled populations may be distributed around just one of the two equilibria – as argued by Aoki (2015).

A standard model of interspecific competition is the Lotka–Volterra (LV) model (Shigesada and Kawasaki, 1997), which tracks size changes in two competing populations. Gilpin et al. (2016) introduced into this framework an interaction between the size and culture level of each of two competing *regional* populations, the Neanderthals and modern humans. Specifically, innovations that raise culture level were assumed more likely to occur in larger populations, and the carrying capacity of each species was assumed to be a function of its culture level. The dynamics of each species in isolation allow bistability as noted above. When both species are considered together, the interaction between population size and culture level produces multiple equilibria, but most importantly allows a population with a higher culture level but a smaller size to outcompete a larger population at a lower culture level.

Spatially explicit mathematical and/or computational models of the invasion by modern humans and their eventual replacement of resident Neanderthals have taken several different forms. In an early model (Flores, 1998), competition of the LV type, with a viability advantage assumed for modern humans, was extended to include diffusion (random non-directional migration) by modern humans (but not the Neanderthals). A sequel model (Flores, 2011) – and a subsequent closely related one (Wang and Lai, 2012) – allowed diffusion by both competing species and gave rise to traveling wave solutions of the type known for the Fisher–KPP equation (Fisher, 1937; Kolmogoroff et al., 1937). In a different vein, Aoki (1998) formulated a reaction–diffusion model assuming culture/technology transfer from modern humans to Neanderthals, which predicted that the Middle Palaeolithic would be replaced by transitional cultures (e.g., Châtelperronian), which in turn would be replaced by the Upper Palaeolithic (Welker et al., 2016).

A spatially explicit computational model for the spread of modern humans into regions occupied by Neanderthals was proposed by Currat and Excoffier (2004, 2011) and Currat et al. (2008). Their model assumes a demographic advantage to modern humans that entails eventual replacement and shows that even a small amount of interbreeding at the wave front would result in massive introgression of Neanderthal genes into modern humans, which is contrary to observation (Green et al., 2010; Reich et al., 2010; Prüfer et al., 2014). They conclude, therefore, that there were obstacles to interbreeding.

The spread of Neolithic farmers across Europe was one of the first archaeological applications of the Fisher–KPP wave of advance model (Ammerman and Cavalli-Sforza, 1971, 1973, 1984), yielding a theoretical prediction for the speed of expansion consistent with the empirical estimate of about 1 km/yr. More complex reaction–diffusion models allowing for conversion of indigenous hunter–gatherers to farming have also been proposed (Aoki et al., 1996).

A modified Fisher–KPP model incorporating a time delay between successive migrations (equivalent to the mean generation time) was subsequently applied to the post-LGM recolonization of Europe by Upper Palaeolithic hunter–gatherers (Fort et al., 2004), where the speed inferred from archaeological data is 0.4–1.1 km/yr. Based on a limited amount of data (Bar-Yosef and Pilbeam, 2000; Stringer et al., 2000; Fort et al., 2004) suggested that the speed of the modern human wave of advance into the Levant and Europe was 0.5 km/yr. With a larger data set of calibrated radiocarbon dates, Mellars (2006a) produced an estimate of perhaps 0.4 km/yr for the rate of spread of modern humans from the Levant into Europe. The latter two estimates pertain to the case where modern humans were invading regions occupied by Neanderthals, as opposed to the former where spread was likely into empty space. Interestingly, the latter two estimates (0.5 km/yr and 0.4 km/yr) are at the lower end of the range of the former (0.4–1.1 km/yr), which is consistent with the theoretical predictions of the diffusive LV competition model (Shigesada and Kawasaki, 1997).

Reaction–diffusion models have also been applied to competition between exploiters and altruists (Wakano, 2006) and to competition between individual and social learners (Wakano et al., 2011).

In the present study we investigate theoretically the spatial spread of modern humans into regions, including non-European Eurasia, occupied by Neanderthals and/or other archaics. Our goals are to obtain the conditions under which the former can replace or assimilate the latter, to predict the speed at which replacement or assimilation will occur given that it does, and to estimate the duration of regional overlap (coexistence) of the two species. To do so, we formulate a reaction–diffusion model that introduces, into our previous model (Gilpin et al., 2016), spatial structure and diffusion between neighboring regions of this space. Our ecocultural model differs from the standard diffusive LV competition model in that the carrying capacities of the competing species are not arbitrarily

Please cite this article in press as: Wakano J.Y., et al., Ecocultural range-expansion scenarios for the replacement or assimilation of Neanderthals by modern humans. Theoretical Population Biology (2017), https://doi.org/10.1016/j.tpb.2017.09.004.

fixed, but can vary at short distances in response to the culture level of the regional population. In other words, we posit a significant effect of the culture levels of modern humans and Neanderthals on the success or failure of the range expansion of the former, through their effect on relative population densities.

More specifically, Gilpin et al. (2016) defined a variable called culture level to quantify culture, where culture level can be interpreted as the number of cultural traits, toolkit size, toolkit sophistication, etc. However, culture level is not an appropriate variable for a reaction–diffusion model, so we quantify culture here in terms of the density of "skilled" individuals – i.e., individuals with a set of useful cultural traits – who form a subset of the population.

A possible example of the kind of skill we have in mind is the know-how and ability to manufacture and use bladelets and microliths. We realize that the advantages afforded by microlithic technologies and their spatial/temporal distribution are contentious issues in archaeology (e.g., Bar-Yosef and Kuhn, 1999; Kuhn, 2002; Eren et al., 2008; Hiscock et al., 2011; Brown et al., 2012; Zwyns et al., 2012; Mellars et al., 2013; Villa and Roebroeks, 2014; Hublin, 2015; Boëda et al., 2015). Nevertheless, we mention it here so as the reader may form a concrete image of what we mean by a skill, deferring the detailed considerations of the question until the Discussion.

For simplicity, the current model ignores interbreeding, which is known to have occurred (Green et al., 2010; Reich et al., 2010; Kuhlwilm et al., 2016), and culture/technology transfer between species, which may or may not have occurred (Bar-Yosef, 2013; Villa and Roebroeks, 2014; Roussel et al., 2016). We also assume a spatially uniform environment, i.e., geomorphological and climatic obstacles to range expansion are not modeled here. Moreover, the distinction between high and low culture levels is, to a first approximation, assumed to apply in all regions.

2. Models

For two competing species in an unstructured habitat, we set

$$\frac{dN_1}{dt} = r_1 N_1 \left(1 - \frac{N_1 + b_{12}N_2}{M_1(Z_1)}\right), \tag{1a}$$

$$\frac{dN_2}{dt} = r_2 N_2 \left(1 - \frac{N_2 + b_{21}N_1}{M_2(Z_2)}\right), \tag{1b}$$

$$\frac{dZ_1}{dt} = r_1 Z_1 \left(1 - \frac{N_1 + b_{12}N_2}{M_1(Z_1)}\right) - \gamma_1 Z_1 + \delta_1 (N_1 - Z_1), \tag{1c}$$

$$\frac{dZ_2}{dt} = r_2 Z_2 \left(1 - \frac{N_2 + b_{21}N_1}{M_2(Z_2)}\right) - \gamma_2 Z_2 + \delta_2 (N_2 - Z_2). \tag{1d}$$

The derivation is given in *Supporting Information* (*SI*) 1 (see Appendix A).

Variables and parameters indexed by 1 and 2 refer to the resident archaics and the intrusive moderns, respectively. The dependent variables are the population density, $N_i(t)$, and the density of skilled individuals, $Z_i(t)$, at time t, where $0 \le Z_i(t) \le N_i(t)$. Each newborn chooses a random member of its population as an exemplar from whom it acquires the skill if that exemplar is skilled. Eqs. (1c) and (1d) are derived assuming random oblique transmission within each species, but the equations and hence the results do not change on assuming that cultural transmission is partly vertical (Cavalli Sforza and Feldman, 1981, p. 84). Skilled individuals then lose their skill at rate γ_i, and unskilled individuals can acquire the skills by innovation at rate δ_i. Loss of skill could be due to, for example, to imperfect recollection, lack of practice, or to cultural drift (Henrich, 2004). In addition, r_i is the intrinsic growth rate, b_{12} and b_{21} are the interspecific competition coefficients, and

$$M_i(Z_i) = \begin{cases} M_{iL} \text{ if } Z_i < Z_i^* \\ M_{iH} \text{ if } Z_i \ge Z_i^* \end{cases} \tag{1e}$$

is the carrying capacity of species i (1 or 2). That is, $M_i(Z_i)$ is step function with a discontinuous upshift from M_{iL} to M_{iH} at the critical density of skilled individuals, Z_i^* (see, e.g., Henrich, 2004; Powell et al., 2009; Ghirlanda and Enquist, 2007, Fig. 1). We will refer to parameter Z_i^* as the "threshold", larger values of which entail that more skilled individuals are required to support the high carrying capacity. More general forms for $M_i(Z_i)$ can be assumed without changing the qualitative behavior of model Eqs. (1a)–(1d) (Aoki, 2015; Gilpin et al., 2016). Importantly, Eq. (1) ignores transfer, either of genes (interbreeding) or of the skills (acculturation), between the two species.

Furthermore, we assume

$$M_{iL} < \frac{Z_i^*}{\theta_i} < M_{iH}, \tag{1f}$$

where $\theta_i = \frac{\delta_i}{\gamma_i + \delta_i}$. The constraint (1f) entails that each species in isolation can exist stably at either the low or the high carrying capacity (bistability). A larger value of parameter θ_i implies greater cognitive (learning) ability, because γ_i and δ_i are the rates of loss and acquisition of the skills by social learning and innovation, respectively. Alternatively, it can mean that the skills are easier to retain or innovate.

We now introduce spatial structure, specifically an infinite one-dimensional space, and diffusion between neighboring regions of this space. Let $N_i(x, t)$ and $Z_i(x, t)$ represent the density of all individuals (population density) and of skilled individuals (skilled density), respectively, of species i (= 1, 2) at location x and time t. With regard to our archaeological example of bladelets/microliths, it seems reasonable to assume that skilled density would be positively correlated with the visibility or abundance of such artefacts in lithic assemblages. We allow for possibly different diffusion coefficients (one-half the mean squared migration distance per unit time) in the two species, D_1 and D_2, and write our reaction–diffusion model as

$$\frac{\partial N_1}{\partial t} = D_1 \frac{\partial^2 N_1}{\partial x^2} + r_1 N_1 \left(1 - \frac{N_1 + b_{12}N_2}{M_1(Z_1)}\right) \tag{2a}$$

$$\frac{\partial N_2}{\partial t} = D_2 \frac{\partial^2 N_2}{\partial x^2} + r_2 N_2 \left(1 - \frac{N_2 + b_{21}N_1}{M_2(Z_2)}\right) \tag{2b}$$

$$\frac{\partial Z_1}{\partial t} = D_1 \frac{\partial^2 Z_1}{\partial x^2} + r_1 Z_1 \left(1 - \frac{N_1 + b_{12}N_2}{M_1(Z_1)}\right) - (\gamma_1 + \delta_1) Z_1 + \delta_1 N_1 \tag{2c}$$

$$\frac{\partial Z_2}{\partial t} = D_2 \frac{\partial^2 Z_2}{\partial x^2} + r_2 Z_2 \left(1 - \frac{N_2 + b_{21}N_1}{M_2(Z_2)}\right) - (\gamma_2 + \delta_2) Z_2 + \delta_2 N_2 \tag{2d}$$

where $M_i(Z_i)$ is given by Eq. (1e) and satisfies inequalities (1f).

We focus on characterizing each traveling wave solution (TWS) of Eq. (2). From anthropologically reasonable initial conditions, multiple traveling wave fronts with different speeds are observed, which originate from several different TWSs of Eq. (2). We will study the directionalities and speeds of these TWSs.

3. Results

3.1. Without spatial structure

3.1.1. Existence and local stability of equilibria

Internal (coexistence of the two species) equilibria of Eq. (1) take the form

$$\hat{N}_1 = \frac{\hat{M}_1 - b_{12}\hat{M}_2}{1 - b_{12}b_{21}},\ \hat{Z}_1 = \theta_1 \hat{N}_1,\ \hat{N}_2 = \frac{\hat{M}_2 - b_{21}\hat{M}_1}{1 - b_{12}b_{21}},\ \hat{Z}_2 = \theta_2 \hat{N}_2, \tag{3}$$

where $\hat{M}_i = M_i(\hat{Z}_i)$ and $\theta_i = \frac{\delta_i}{\gamma_i+\delta_i}$. Existence requires $\hat{N}_1 > 0, \hat{N}_2 > 0$ and that the consistency condition

$$\hat{N}_i < \frac{Z_i^*}{\theta_i} \text{ when } \hat{M}_i = M_{iL} \tag{4a}$$

$$\hat{N}_i \geq \frac{Z_i^*}{\theta_i} \text{ when } \hat{M}_i = M_{iH} \tag{4b}$$

be satisfied. Each such equilibrium is locally stable if $b_{12}b_{21} < 1$. Since $\hat{M}_i = M_{iL}$ or M_{iH}, up to four internal equilibria of the form in Eq. (3) may exist.

Edge (exclusion of one species by the other) equilibria of the form

$$\hat{N}_1 = \hat{M}_1,\ \hat{Z}_1 = \theta_1\hat{M}_1,\ \hat{N}_2 = 0, \hat{Z}_2 = 0, \tag{5a}$$

or

$$\hat{N}_1 = 0, \hat{Z}_1 = 0, \hat{N}_2 = \hat{M}_2\hat{Z}_2 = \theta_2\hat{M}_2, \tag{5b}$$

also exist given inequalities (1f), and are locally stable if $b_{21} > \frac{\hat{M}_2}{\hat{M}_1}$ and $b_{12} > \frac{\hat{M}_1}{\hat{M}_2}$, respectively. Since $\hat{M}_i = M_{iL}$ or M_{iH}, there are a total of four edge equilibria. The zero equilibrium (extinction of both species) exists and is unstable.

It is shown in *SI* 2 that $Z_i(t)$ converges to $\theta_i N_i(t)$ from all initial conditions that satisfy $N_i(0) > 0$.

3.1.2. Special case of cognitive and intrinsic-demographic equivalence with partial niche overlap

We consider here the special case when all parameter values are identical in the two species, which entails cognitive and intrinsic-demographic equivalence of Neanderthals and modern humans. Moreover, we assume *partial* overlap of the niches (Banks et al., 2008; Hoffecker, 2009; Roebroeks and Soressi, 2016) of the two species and correspondingly set $b_{12} = b_{21} = b < 1$.

We use the shorthand notation

$$E_{LL} = \left(\frac{M_L}{1+b}, \frac{M_L}{1+b}\right) \tag{6a}$$

$$E_{LH} = \left(\frac{M_L - bM_H}{1-b^2}, \frac{M_H - bM_L}{1-b^2}\right) \tag{6b}$$

$$E_{HL} = \left(\frac{M_H - bM_L}{1-b^2}, \frac{M_L - bM_H}{1-b^2}\right) \tag{6c}$$

$$E_{HH} = \left(\frac{M_H}{1+b}, \frac{M_H}{1+b}\right) \tag{6d}$$

to denote the four internal equilibria. The first and second quantities in the parentheses on the right hand sides of Eq. (6) are the values of $\hat{N}_1$ and $\hat{N}_2$, respectively, obtained by setting $M_{1L} = M_{2L} = M_L$, $M_{1H} = M_{2H} = M_H$, and $b_{12} = b_{21} = b$ in Eq. (3). The densities of skilled individuals at these equilibria are then $\hat{Z}_1 = \theta\hat{N}_1$ and $\hat{Z}_2 = \theta\hat{N}_2$, where $\theta_1 = \theta_2 = \theta$. We will refer to E_{LL} and E_{HH} as the low and high symmetrical internal equilibria, respectively, and to E_{LH} and E_{HL} as the asymmetrical internal equilibria.

Similarly, we write the four edge equilibria as

$$E_{L0} = (M_L, 0) \tag{7a}$$

$$E_{0L} = (0, M_L) \tag{7b}$$

$$E_{H0} = (M_H, 0) \tag{7c}$$

$$E_{0H} = (0, M_H)\,. \tag{7d}$$

Here, E_{L0} and E_{0L} are the low edge equilibria, whereas E_{H0} and E_{0H} are the high edge equilibria.

Combining our basic assumption inequalities (1f) with the simplifying assumptions made here, we find that the low edge equilibria, E_{L0} and E_{0L}, exist but are unstable. For the other equilibria, we can distinguish two cases. First, if $M_L < \frac{Z^*}{\theta} < \frac{M_H}{1+b}$ and $0 < b < \frac{M_L}{M_H}$, all four internal equilibria, E_{LL}, E_{LH}, E_{HL}, and E_{HH}, exist and are locally stable; then both high edge equilibria, E_{H0} and E_{0H}, are unstable (Fig. 1 panel A). Second, if $M_L < \frac{Z^*}{\theta} < \frac{M_H}{1+b}$ and $\frac{M_L}{M_H} < b < 1$, then both symmetrical internal equilibria, E_{LL} and E_{HH}, as well as both high edge equilibria, E_{H0} and E_{0H}, exist and are locally stable; under these conditions the asymmetrical internal equilibria, E_{LH} and E_{HL}, do not exist (Fig. 1 panel B).

Fig. 1 plots these equilibria in the (N_1, N_2)−plane, on the assumption that $Z_1(t)$ and $Z_2(t)$ have converged to $\theta N_1(t)$ and $\theta N_2(t)$, respectively. It can be shown that the basins of attraction of the four locally stable equilibria in each of the two cases distinguished above are the four rectangular regions bounded by a vertical dashed line at $N_1 = Z^*/\theta$ and a horizontal dashed line at $N_2 = Z^*/\theta$. As discussed in Section 3.2.3, the directionality of a TWS connecting two locally stable equilibria (i.e., a *bistable* wave) is determined by the locations of these thresholds relative to the locations of these equilibria.

3.2. With spatial structure

3.2.1. A special solution of Eq. (2)

We show in *SI* 2 that, if Eq. (2) has a solution, then a special solution of the form

$$\begin{aligned} Z_1(x,t) &= \theta_1 N_1(x,t) \\ Z_2(x,t) &= \theta_2 N_2(x,t) \end{aligned} \tag{8}$$

exists, which is globally stable (for demographically relevant solutions). Convergence to the solution in Eq. (8) entails that the number of dependent variables can be reduced from four to two, as a result of which the null cline analysis illustrated in Fig. 1 to interpret the dynamics without spatial structure remains useful in studying the dynamics with spatial structure.

3.2.2. Eigenstructure analysis at an edge equilibrium and the minimum speed of a TWS

In *SI* 3, we derive the minimum possible speed of a TWS that connects an edge equilibrium Eq. (5b) (where $\hat{N}_1 = 0$) to an internal (coexistence) equilibrium Eq. (3), which is

$$|v| \geq 2\sqrt{D_1 r_1\left(1 - b_{12}\frac{\hat{M}_2}{\hat{M}_1}\right)}. \tag{9a}$$

The minimum speed is important as it often, though not necessarily, corresponds to the realized speed, which is estimated by numerical analysis, of a TWS (Shigesada and Kawasaki, 1997). However, without further information, we cannot determine whether v is positive or negative – the wave front may move right or left, respectively – so "minimum" here refers to the absolute value of the speed. Nevertheless, inequality (9a) defines a non-zero minimum speed only if $b_{12} < \frac{\hat{M}_1}{\hat{M}_2}$, in which case the edge equilibrium Eq. (5b) is unstable. Hence, if the internal equilibrium Eq. (3) to which the TWS is connected is locally stable, we have by definition a *monostable* wave, and its directionality is such that the spatial regions where equilibrium Eq. (5b) (with $\hat{N}_1 = 0$) holds contract.

Similarly, the minimum speed of a TWS that connects an edge equilibrium Eq. (5a) (where $\hat{N}_2 = 0$) to an internal (coexistence) equilibrium Eq. (3) is given by

$$|v| \geq 2\sqrt{D_2 r_2\left(1 - b_{21}\frac{\hat{M}_1}{\hat{M}_2}\right)}. \tag{9b}$$

Inequality (9b) defines a non-zero minimum speed only if $b_{21} < \frac{\hat{M}_2}{\hat{M}_1}$, in which case the edge equilibrium Eq. (5a) is unstable.

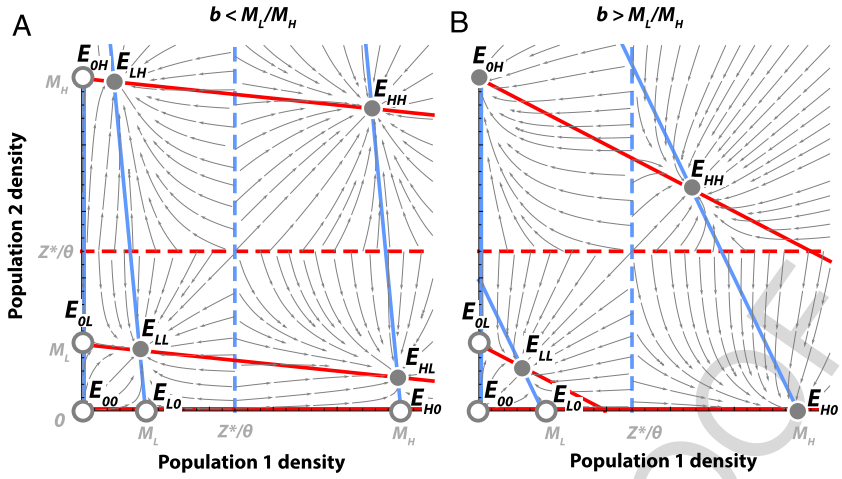

Fig. 1. Dynamics of Eq. (1) in the (N_1, N_2)-plane. Parameter values are equal in the two species. $Z_i(t) = \theta N_i(t)$ is assumed. Solid lines indicate the null clines $\frac{dN_i}{dt} = 0$. The dashed vertical and horizontal lines indicate the thresholds $N_i = Z^*/\theta$ where the carrying capacities jump between M_L and M_H. Blue and red refer to species $i = 1$ and 2, respectively. Intersections of two null clines correspond to locally stable (filled circles) and unstable (open circle) equilibria. Equilibria emphasized in the text are labelled. Trajectories are indicated by thin lines with arrowheads. We set $b = 0.1$ in panel A and $b = 0.5$ in panel B. Other parameter values are $\theta = 0.5, Z^* = 12, r = 1, M_L = 10, M_H = 50$. (For interpretation of the references to color in this figure legend, the reader is referred to the web version of this article.)

3.2.3. Direction of travel of a bistable wave

A bistable wave connects two locally stable equilibria of Fig. 1. Unlike the monostable wave the speed of bistable wave is uniquely determined. However, we are unable to derive it mathematically, and we obtain instead an approximate condition that predicts its directionality, i.e. whether it is positive, zero, or negative.

For simplicity, we consider only the situation analyzed in Section 3.1.2 with identical parameter values assumed for both species. Fig. 1 panel A illustrates the case where all four internal equilibria are locally stable. Consider a TWS connecting the two locally stable internal equilibria E_{LH} and E_{LL}. Assume as in Fig. 2 panel A that E_{LH} holds to the left of the wave front and E_{LL} to the right. As shown in *SI* 4, an approximate condition for the spatial regions where E_{LH} holds to expand at the expense of the regions where E_{LL} holds is

$$2\left(\frac{(1-b^2)Z^*}{\theta}\right)^3 + 3bM_L\left(\frac{(1-b^2)Z^*}{\theta}\right)^2 - M_L\left(M_H^2 + (1-3b)M_HM_L + b^3M_L^2\right) < 0. \quad (10a)$$

For given values of M_L, M_H, and b, the critical value of Z^*/θ that predicts zero speed can be obtained by numerically solving the cubic Eq. (10a) (black triangle in Fig. 3A).

A similar analysis can be done for a TWS connecting the locally stable edge equilibrium, E_{0H}, and the locally stable internal equilibrium, E_{LL}. When the configuration of null-clines is as in Fig. 1 panel B, which occurs when $M_L < Z^*/\theta$ and $\frac{M_L}{M_H} < b < 1$, an approximate condition for the spatial regions where E_{0H} holds to expand at the expense of the regions where E_{LL} holds (Fig. 2 panel B) is

$$2b(1+b)^2(M_H - M_L)\left(\frac{Z^*}{\theta}\right)^3 - b(1+b)^2M_H^3M_L + (1+3b)M_L^3M_H < 0 \quad (10b)$$

(black triangle in Fig. 3B).

3.3. Numerical analysis

Numerical simulations of Eq. (2) were performed on the finite spatial domain $0 \le x \le L$ with zero-flux boundary conditions. Our purpose here is to investigate the conditions under which modern humans could have replaced or assimilated the archaic humans, even if as claimed by some archaeologists their cognitive (learning) capabilities did not differ (e.g., Zilhão et al., 2010; Villa and Roebroeks, 2014; Roebroeks and Soressi, 2016). Hence, we equate the three parameters related to cognition in the two species: $\gamma_1 = \gamma_2 = \gamma, \delta_1 = \delta_2 = \delta, Z_1^* = Z_2^* = Z^*$. Since we also wish to explore whether an intrinsic demographic superiority of modern humans is a necessary condition for replacement or assimilation, we set all demographic parameters equal in the two species: $r_1 = r_2 = r, M_{1L} = M_{2L} = M_L, M_{1H} = M_{2H} = M_H, D_1 = D_2 = D, b_{12} = b_{21} = b$.

On the other hand, we posit an advantage to modern humans in the initial conditions. Invoking bistability of regional populations in isolation – i.e., $M_L < Z^*/\theta < M_H$ (inequalities (1f)) – we assume that due to historical contingency modern and archaic humans were distributed throughout Africa and Eurasia at the high and low carrying capacities, respectively. This assumption of disparate initial densities is informed by available genetic and archaeological estimates of the effective and census population sizes of Neanderthals and modern humans at around the time of the latter's out-of-Africa dispersal (Bocquet-Appel et al., 2005; Atkinson et al., 2009; Mellars and French, 2011; Bocquet-Appel and Degioanni, 2013; Villa and Roebroeks, 2014; Prüfer et al., 2014; Kuhlwilm et al., 2016). Specifically, representing the spatial extent of Africa and Eurasia by the left and right halves of our finite spatial domain $0 \le x \le L$, we set

$$N_1(x,0) = 0, N_2(x,0) = M_H \text{ for } 0 \le x \le \frac{L}{2} \quad (11a)$$

$$N_1(x,0) = M_L,\ N_2(x,0) = 0 \text{ for } \frac{L}{2} < x \le L \quad (11b)$$

$$Z_1(x,0) = \theta N_1(x,0) \text{ for } 0 \le x \le L \quad (11c)$$

$$Z_2(x,0) = \theta N_2(x,0) \text{ for } 0 \le x \le L. \quad (11d)$$

The skilled densities were always seen to converge to the quasi-equilibrium values, $Z_i(x,t) = \theta N_i(x,t)$, whether or not conditions (11c) and (11d) were imposed at the start of the simulation.

It may be special pleading to assume that all modern human and archaic regional populations would initially have been at the high and low carrying capacities, respectively, due in effect to chance. Later we show that relaxing the stringent condition Eq. (11) does not significantly affect our results, but first we describe the basic

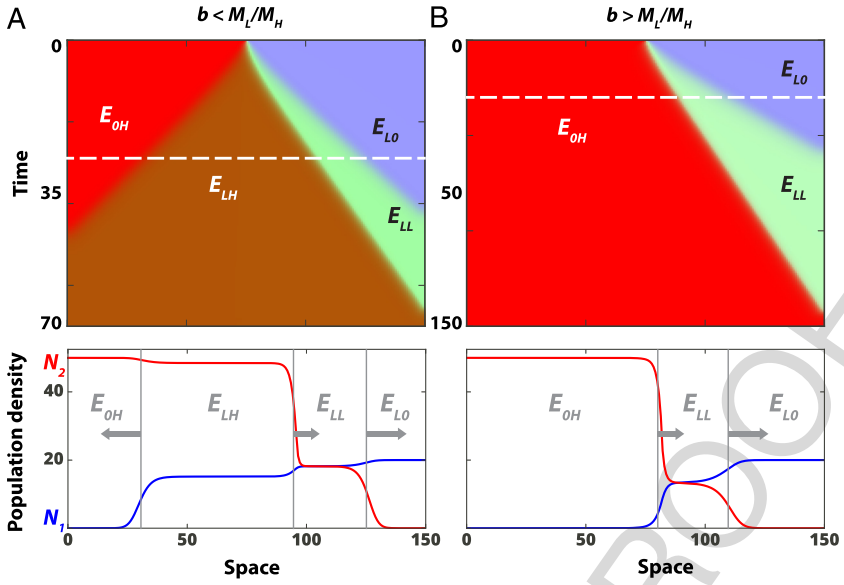

Fig. 2. Numerical solutions of Eq. (2) on the finite spatial domain. Parameter values are equal in the two species. (Upper) Kymographs showing the evolution of the system Eq. (2) from the spatially-segregated initial conditions Eq. (11). Time on the vertical axis is measured downward and stops when the second wave front reaches the right boundary. At any previous moment, the densities in different regions of space are close to the following equilibria: exclusion of species 1 (Eq. (7c)) and species 2 (Eq. (7a)) as indicated by red and blue shading, respectively; low symmetrical coexistence of the two species (Eq. (6a)) as indicated by green shading; and asymmetrical coexistence with species 2 at the higher density (Eq. (6b)) as indicated by brown shading. Qualitatively different types of invasion – assimilation when $b = 0.1$ (panel A) and replacement when $b = 0.5$ (panel B) – are observed. (Lower) Snapshots of the wave profiles at the time indicated by white dashed horizontal lines on the kymographs above, with directionalities indicated by gray arrows and their relative speeds by the lengths of these arrows. Other parameter values are $\gamma = \delta = 0.2, Z^* = 11, r = 1, D = 1, M_L = 20, M_H = 50$. (For interpretation of the references to color in this figure legend, the reader is referred to the web version of this article.)

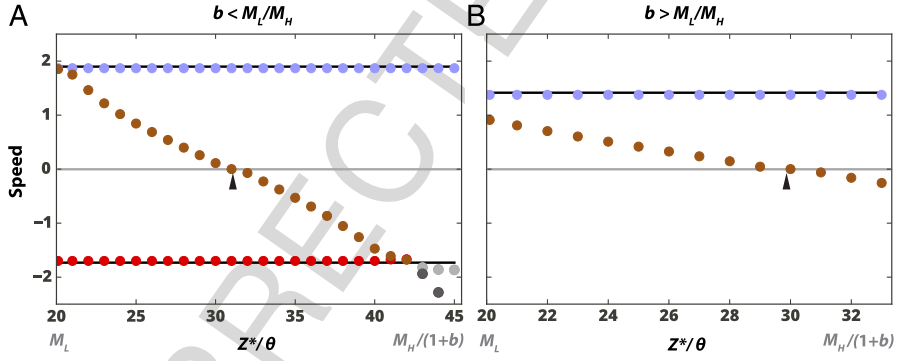

Fig. 3. Dependence of the speeds of the wave fronts on Z^*/θ (ratio of the threshold density of skilled individuals to cognitive ability). Numerically-determined speeds of the wave fronts for the two strengths of competition shown in the previous figure, $b = 0.1$ (A) and $b = 0.5$ (B). The speeds of the first, second, and third waves are indicated by blue, brown, and red discs, respectively. Analytical predictions for the minimum speeds are indicated by solid lines, when known (Eqs. (12a) and (12b)). Only the speed of the second wave depends on Z^*/θ. Note this speed does not depend on Z^* and θ individually, because it is measured after convergence to Eq. (8). Assimilation (A) or replacement (B) can only occur when the speed of this second wave is greater than zero, which can be predicted analytically (black triangle, Eqs. (10a) and (10b)). Since this speed is negatively correlated with Z^*/θ, the duration of low coexistence (equilibrium E_{LL}) is shorter for smaller values of Z^*/θ. Gray discs give the speeds of a qualitatively different solution with a wave profile that differs from those illustrated in Fig. 2 (Supporting Fig. 4). Fixed parameter values are $\theta = 0.5, r = 1, D = 1, M_L = 20, M_H = 50$. (For interpretation of the references to color in this figure legend, the reader is referred to the web version of this article.)

scenarios of replacement and assimilation that are predicted under this condition.

Due to the assumed difference in initial densities, we never observe extinction of modern humans in the numerical simulations. The demographically "worst" scenario for modern humans is represented by a solution such that E_{LL} eventually displaces all other equilibria and, in particular, such that the initially high density of modern humans at the left of the spatial domain collapses (see below). In other words, modern and archaic humans are predicted eventually to coexist at the same low density $\frac{M_L}{1+b}$ throughout Africa and Eurasia. We may take this scenario as the default case against which the effects of altering the parameter values may be compared. In what follows, we assume $M_L < \frac{Z^*}{\theta} < \frac{M_H}{1+b}$.

3.4. Assimilation scenario

When $0 < b < \frac{M_L}{M_H}$, three wave fronts, two monostable and one bistable, form spontaneously after an initial transient. Fig. 2A lower panel shows a snapshot of the wave profiles. The monostable wave front at the right (the first wave) travels toward the right (i.e., with positive speed), with the result that the low coexistence equilibrium, E_{LL} (Eq. (6a)), replaces the low edge equilibrium, E_{L0} (Eq. (7a)). This wave front represents the expansion of a relatively small number of modern humans into regions previously occupied solely by Neanderthals, and is shown in Fig. 2A upper panel as a transition from blue to green. The observed speed is in good agreement with the analytically-derived minimum speed Eq. (9b),

which reduces here to

$$v = 2\sqrt{Dr\,(1-b)}. \tag{12a}$$

In the example illustrated in Fig. 2, the bistable wave front in the middle (the second wave) represents the further expansion of modern humans such that in its wake they exist at a higher density than the Neanderthals. This wave front moves toward the right (i.e., with positive speed) because inequality (10a) is satisfied here. Hence, the asymmetric coexistence equilibrium, E_{LH} (Eq. (6b), brown shading in Fig. 2A upper panel), replaces the low coexistence equilibrium, E_{LL} (Eq. (6a), green). For the parameter values considered in this paper, however, the second wave is slower than the first wave, which entails that low coexistence lasts longer at regions that are closer to the periphery of the spatial domain (compare the lengths of the vertical transects through the green triangle in Fig. 2A upper panel).

As Z^*/θ approaches $\frac{M_H}{1+b}$ from below, inequality (10a) no longer holds, the speed becomes negative (Fig. 3 panel A), and we observe the default case. From Fig. 1 panel A, we see that Z^*/θ is the horizontal threshold between the domains of attraction of E_{LH} and of E_{LL} in the $(N_1, N_2)-$plane. The intuitive reason why relatively large values of Z^*/θ are associated with negative speeds of the second wave is that this threshold is pushed upward, so that the latter domain of attraction becomes larger. A negative speed means that E_{LH} is replaced by E_{LL}.

Finally, the monostable wave front at the left (third wave) travels toward the left (i.e., with negative speed) and represents the expansion of a relatively small number of Neanderthals into regions where modern humans were resident. That is, the asymmetric coexistence equilibrium, E_{LH} (Eq. (6b), brown), replaces the high edge equilibrium, E_{0H} (Eq. (7d), red). The observed speed is in good agreement with the analytically-derived minimum speed Eq. (9a), which reduces here to

$$v = -2\sqrt{Dr\left(1-b\frac{M_H}{M_L}\right)}. \tag{12b}$$

We call the pattern of events when the second wave has positive speed the "assimilation" scenario, because a relatively small number of archaics remains after invasion by moderns, and although not explicitly modeled, the former would by interbreeding be absorbed into the latter. Interestingly, as Fig. 2A lower panel shows, four different equilibria of Eq. (1) are simultaneously visible in the simulation in separate regions of the one-dimensional domain – from left to right E_{0H}, E_{LH}, E_{LL}, E_{L0} – with smooth spatial gradients monotonically interpolating between these equilibria.

To summarize, when $0 < b < \frac{M_L}{M_H}$ and Z^*/θ is sufficiently small, our analysis predicts the assimilation of Neanderthals by modern humans. Importantly, it is the directionality of the second wave in our ecocultural model that determines whether assimilation will occur (positive speed in Fig. 3 panel A). This assimilation scenario, however, entails that Neanderthals would have contributed to the ancestry of Africans as well as Eurasians, a prediction that is currently not supported by genetic studies.

3.5. Replacement scenario

When interspecific competition is stronger, with $\frac{M_L}{M_H} < b < 1$, a transcritical bifurcation occurs in Eq. (1) such that the asymmetric coexistence equilibria (Eqs. (6b), (6c)) become unstable, but the high edge equilibria (Eqs. (7c), (7d)) are now locally stable. This qualitatively changes the wave profiles, such that only one monostable and one bistable wave front now occur. For the parameter values assumed in Fig. 2B, both travel toward the right (i.e., with positive speed). Moreover, the monostable first wave has an observed speed that agrees with the analytically-derived minimum Eq. (12a).

The bistable second wave represents the complete replacement of Neanderthals by modern humans. We call this the "replacement" scenario. As in the previous case of $0 < b < \frac{M_L}{M_H}$, low coexistence lasts longer at regions that are closer to the periphery of the spatial domain (see also Fig. 4). For larger values of Z^*/θ than is assumed in Fig. 2B, the speed of the second wave is negative (Fig. 3 panel B), and we again observe the default case. In this case, replacement does not occur.

In summary, when $\frac{M_L}{M_H} < b < 1$ and Z^*/θ is sufficiently small, our analysis predicts the replacement of Neanderthals by modern humans. It is the directionality of the second wave that again determines whether replacement, in this case, can occur (Fig. 3 panel B).

3.6. Critical level of niche overlap

In both assimilation and replacement scenarios, carrying capacities of both species are low in the first wave, while increased carrying capacity associated with cultural difference drives the second wave. The first wave is due to ecological invasion by moderns who exploit the niche that is not used by Neanderthals. Thus, when niche overlap is larger (i.e., b is closer to 1), the first wave becomes slower (see Eq. (12a)). The second wave is a cultural invasion by moderns who utilize their increased carrying capacity, which is supported by high skilled density. Thus, the speed of the second wave is faster when the advantage of culture (M_H/M_L) is larger or when transition to a higher carrying capacity is more likely to occur (Z^*/θ is smaller). Keeping these culture-related parameters constant, the first wave could be slower than the second wave when b is close to 1. This speculation is consistent with the analytic result of the special case $b \to 1$, where the speed of the first wave is zero (Eq. (12a)), while the speed of the second wave can be still positive (inequality (10b) holds when M_H/M_L is sufficiently large). The speculation is also supported by numerical calculations for $b > 0.95$ (Supporting Fig. 3), in which case the first and second waves coincide to form a single wave (profiles not shown). Intuitively, if the two species' niches are almost identical, ecological invasion is nearly impossible and cultural difference becomes the major reason for invasion of Neanderthals by moderns. If niche difference is small but not negligible, then we observe wave profiles as shown in Fig. 2B. Although we set a large advantage of culture ($M_H/M_L = 50/20$), our numerics showed that a low coexistence region of modern humans and Neanderthals appears and expands even for relatively high niche overlap ($b = 95\%$).

3.7. Local overlap in the replacement scenario

Interbreeding of Neanderthals and modern humans requires that they overlap locally, and opportunities for interbreeding would likely increase with the spatial extent and duration of this local overlap. In the replacement scenario of our model, the two species overlap locally in regions in and around where the low symmetrical coexistence equilibrium, E_{LL}, holds (Fig. 2B lower panel). Hence, the duration of local overlap at any given location in space roughly corresponds to the length of time that this equilibrium holds there. This is shown in Fig. 4 as a function of distance from the site of initial interaction. Because, over long enough distances, the wave fronts propagate with constant speed, any given location in space will encounter the wave fronts in descending order of their relative speeds. Local overlap occurs between the times when modern humans first arrive at a location solely occupied by Neanderthals and when Neanderthals are fully excluded. Hence, the duration of local overlap can be approximated by a function of the relative speeds, $\tau_{overlap}(x) = (x - L/2)\left(1/v_{replace} - 1/v_{coexist}\right)$, where $v_{coexist}$ is the speed of the first wave of arriving modern humans (interface between E_{L0} and E_{LL}), and $v_{replace}$ is the speed

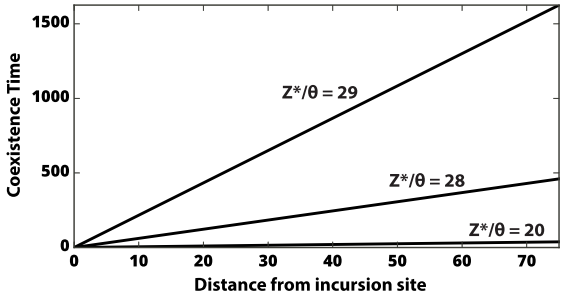

Fig. 4. Duration of local coexistence before eventual replacement depends on the distance from incursion site. Species 1 and 2 coexist at a relatively low density (low coexistence equilibrium E_{LL}) for a longer time at sites farther removed from the initial boundary between the distributions of the two species ($x = L/2$ in Eq. (11)). Parameter values are $r = 1$, $D = 1$, $M_L = 20$, $M_H = 50$, $b = 0.5$, which entail eventual replacement of species 1 by species 2.

of the second wave that fully excludes the Neanderthals (interface between E_{LL} and E_{0H}). The slope of the trend lines in Fig. 4 increase with Z^*.

Local overlap is also observed in the assimilation scenario (Fig. 2A lower panel).

In both the assimilation and replacement scenarios, but especially in the latter, the population and skilled densities of both species are low in the region of local overlap, where E_{LL} holds. The skilled densities here are $\hat{Z}_1 = \hat{Z}_2 = \theta M_L/(1+b)$ (see Eqs. (6a), (8)), which are smaller for the relatively greater values of the competition coefficient, b, that imply replacement. Hence, any artefacts that rely on this skill for their manufacture would arguably be made in small quantities, if at all. It is only in the wake of the second wave that the skilled density of modern humans increases to high levels. Neanderthal skilled density remains low in both scenarios.

3.8. Alternative initial conditions

As an example of initial conditions for which the regional populations of species 2 are not all at the high carrying capacity, consider

$$N_1(x,0) = 0, N_2(x,0) = M_L \text{ for } 0 \le x \le \frac{L}{4} \tag{13a}$$

$$N_1(x,0) = 0, N_2(x,0) = M_H \text{ for } \frac{L}{4} < x \le \frac{L}{2} \tag{13b}$$

$$N_1(x,0) = M_L,\ N_2(x,0) = 0 \text{ for } \frac{L}{2} < x \le L \tag{13c}$$

with $Z_1(x,0)$ and $Z_2(x,0)$ given by Eqs. (11c) and (11d), respectively. In the left half of the spatial domain where only species 2 initially resides, a one-species bistable wave connecting $N_2 = M_L$ and $N_2 = M_H$ will form spontaneously if each of the regions is large enough. Using an argument analogous to that used in deriving Eq. (10a) or (10b), we can show that this bistable wave will travel toward the left if

$$\frac{Z^*}{\theta} < \left[\frac{M_L M_H (M_L + M_H)}{2}\right]^{1/3}, \tag{14}$$

in which case we effectively recover the initial conditions Eq. (11). Focus now on the replacement scenario and consider the relative magnitudes of the critical values of Z^*/θ in inequality (10b) and inequality (14). Then it can readily be shown that the bound in inequality (10b) is smaller (more stringent) than that in inequality 14 (*SI* 4). Hence, we conclude that when replacement is predicted under the initial conditions Eq. (11), i.e., when inequality (10b) is satisfied, it will also occur under the initial conditions (13).

Another interesting example of alternative initial conditions takes the population densities of both species to be in equilibrium at the low carrying capacity,

$$N_1(x,0) = 0, N_2(x,0) = M_L \text{ for } 0 \le x \le \frac{L}{2}, \tag{15a}$$

$$N_1(x,0) = M_L,\ N_2(x,0) = 0 \text{ for } \frac{L}{2} < x \le L, \tag{15b}$$

and $Z_1(x,0)$ to be given by Eq. (11c), but $Z_2(x,0)$ to be greater than Eq. (11d). In the regions distant from the boundary of the two species, the competition and diffusion terms in Eq. (4) can be ignored due to the rarity of the rival species and approximate flatness of the spatial gradients. We argue in *SI* 1 (section below Eq. A2) that, if $Z^* < Z_2(x,0) \le M_L$ for $0 \le x \le L/2$ (or in a substantial part of this range), then we may again effectively recover the initial conditions Eq. (11). This is particularly true when the timescale of demographic change is shorter than that of cultural change, i.e., when $r > \gamma + \delta$, as previously shown by Gilpin et al. (2016).

4. Discussion

An important result of our previous theoretical analysis (Gilpin et al., 2016) was that a large population of Neanderthals may be invaded and overwhelmed by a smaller population of modern humans with a higher culture level, even if the two species did not differ in innate cognitive ability or demographic potential. There was no spatial structure in this previous model, the main properties of which are summarized in Fig. 1 of the current paper, but we suggested there that the replacement process could be self-perpetuating. Here we use a reaction–diffusion framework to explicitly investigate the range expansion of modern humans into regions occupied by Neanderthals. The spatially structured habitat modeled here and the form of the diffusion we assume require that, instead of tracking the culture levels, we focus on the densities of skilled individuals and how these densities affect the dynamics of competition between the two species.

Our ecocultural model Eq. (2) has parallels with the diffusive LV competition model (*SI* 5; Shigesada and Kawasaki, 1997; Hosono, 1998), but importantly differs in one key assumption. The divergent assumption is that the carrying capacity of each species is not arbitrarily fixed, but depends on the density of skilled individuals, which in turn depends on the population density. As a result, the ecocultural model predicts a wave profile with an expanding region of local overlap (i.e., the low symmetrical coexistence region, E_{LL}; Fig. 2 lower panels) in which both species coexist at low constant densities until the dominating high density wave of modern humans arrives. Replacement and assimilation are both possible consequences of the LV model – in fact, they can sometimes occur under less stringent conditions (*SI* 5) – but such a wave profile is not seen in the diffusive LV model. One implication is that two-way genetic exchange may occur in this region of local overlap, as opposed to unidirectional genetic transfer from the resident Neanderthals to the invading modern humans at a wave front where the latter are increasing at the expense of the former (Currat and Excoffier, 2004). Another implication is that the bottleneck experienced by out-of-Africa moderns (Kuhlwilm et al., 2016) may have been caused by interspecific competition.

Over the past fifteen years there have been many attempts to relate population size to culture level using dynamical models. In most of these models, population size is considered as a parameter (Shennan, 2001; Henrich, 2004; Powell et al., 2009; Strimling et al., 2009; Mesoudi, 2011; Lehmann et al., 2011; Kobayashi and Aoki, 2012; Fogarty et al., 2015, in press), and larger population size is generally shown to predict a higher culture level. The models that lead to this prediction have been criticized on two grounds:

first, the assumptions of the models are implausible (Vaesen et al., 2016), and second, the prediction that cultural complexity is governed by population size is not supported by ethnographic or archaeological evidence (Vaesen et al., 2016; Collard et al., 2016). Our analysis can be viewed as an investigation of how population size differences between Neanderthals and modern humans may have arisen and, in particular, how the two-way interaction between culture level or prevalence of culturally transmitted skills could have produced demographic differences (see also Lee, 1986; Ghirlanda and Enquist, 2007; Aoki, 2015; Gilpin et al., 2016). Social factors (rather than cognitive or ecological ones) have also been invoked to explain the eventual dominance of modern humans (Horan et al., 2005).

The replacement scenario of our model predicts a first wave of invading modern humans with low population and skilled densities, which is followed by a slower second wave with high population and skilled densities. When the skilled density is low, any artefacts that rely on this skill for their manufacture and use would arguably be made in small quantities and may not be archaeologically visible. In light of these predictions, it is noteworthy that several archaeologists have suggested a scenario of Neanderthal extinction in the face of two major waves of modern human expansion into Europe, which differ from each other in cultural/behavioral patterns (Bar-Yosef, 2007; Hoffecker, 2009; Hublin, 2015).

The first wave is represented by lithic assemblages grouped as the Bohunician and Bachokirian industries in central and eastern Europe, which are considered to have been produced by modern humans who expanded their range from the Levant, where a similar cultural entity, the Emiran, occurred coevally (Škrdra, 2003; Bar-Yosef and Belfer-Cohen, 2013). These cultural entities are chrono-culturally termed the Initial Upper Palaeolithic (IUP), which are characterized by Upper Palaeolithic tool types, such as end scrapers and burins. However, it is widely known that the IUP core-reduction technology retains some elements of the Levallois method that was prevalent, along with the use of hard hammers, in the Middle Paleolithic, yielding robust blades with large, faceted striking platforms. In addition, only a few IUP sites in Europe and the Levant have yielded bone artifacts and ornaments (Kuhn et al., 2009), leading Hoffecker (2009) to point out "the scarcity of evidence for innovative technology" as "one of the striking characteristics" of the Bohunician industry.

Similar lithic assemblages are also distributed in the southern Altai and Mongolia (Kuhn and Zwyns, 2014). Although the IUP sites discovered so far have not yielded unambiguous modern human fossils, the presence of a contemporaneous 45,000-year-old modern human at Ust'-Ishim in western Siberia suggests that the IUP in southern Siberia can be attributed to modern humans (Fu et al., 2014). During the IUP, Neanderthals were still present in western Europe, where numerous Mousterian sites are distributed coevally (Higham et al., 2014). Hublin (2015) has characterized the IUP of "southwest Asia, eastern and central Europe, and …central Asia" as "a first expansion of modern humans into Eurasia that may have been partly unsuccessful".

A second wave of modern humans has been suggested for the occurrences of the Protoaurignacian industry in Europe and the Early Ahmarian in the Levant, assuming the derivation of the former from the latter by the range expansion of modern humans from the Levant to Europe (Bar-Yosef, 2007; Zilhão, 2007; Hoffecker, 2009; Hublin, 2015; but see Kadowaki et al., 2015). Both industries are characterized by abundant bladelets produced from prismatic cores with soft hammers that create small butts, marking a fully Upper Palaeolithic technology, i.e., the Early Upper Palaeolithic (EUP). Similar bladelet assemblages are also known from the Zagros and the Caucasus regions (Hublin, 2015). These bladelet assemblages are often associated with bone/antler implements and ornaments, which are also typical of the Upper Palaeolithic. Regarding the makers of the Protoaurignacian and the Ahmarian, there are cases in which modern human fossils have been recovered in association with artefact remains (Bergman and Stringer, 1989; Benazzi et al., 2015). In addition, the greater number of sites of the Protoaurignacian and Early Ahmarian in comparison with the IUP sites may indicate an increase in population (Zilhão, 2007; Kadowaki, 2013). In Europe, the Protoaurignacian overlaps in time with the last Mousterian sites (Banks et al., 2013; Higham et al., 2014) and is considered to represent "a cause (either directly or indirectly) of the extinction of the Neanderthals" (Benazzi et al., 2015).

We argue that these two waves of modern human range expansions, empirically observed in fossil and artifact records, could, to a first approximation, correspond to the two waves predicted by our theoretical model. However, our ecocultural model does not equate the skill with any specific lithic industry. We suggest that a possible candidate for the skill may be the know-how and ability to manufacture bladelets/microliths, which requires us to address two questions: (1) what are the advantages associated with bladelets/microliths as opposed to other, larger, tools, and (2) does the spatial/temporal distribution of bladelets/microliths in the archaeological record agree with the proposed routes and timing of modern human dispersal(s)? The first question can only be answered speculatively. Smaller cutting tools, such as bladelets/microliths, may have permitted more economical use of stone (Eren et al., 2008) and may have increased hunting efficiency as armatures of composite projectiles (Shea, 2006). The use of bladelets/microliths as components may have allowed the production of diverse composite tools that aided the exploitation of broader resources (Kuhn, 2002), particularly when the availability of resources was uncertain due to environmental variability (Hiscock et al., 2011).

With regard to the second question, the spread of geometric microliths from their origin in Africa to India and Sri Lanka via the coastal route, as argued by Mellars et al. (2013), may be an exemplary case (but see Petraglia et al., 2007). According to Mellars et al. (2013), the geometric microliths that first appear in southern Asia 40–35 kya are homologous to the Howiesons Poort geometric microliths and were introduced by modern humans dispersing out-of-Africa 60–50 kya. The apparent delay in reaching southern Asia is plausibly attributed to the subsequent rise in sea level that has submerged the earlier archaeological sites (the same explanation may apply to their absence in the intermediate regions along the coastal route). The prediction from our model that the first wave of incoming modern humans would be characterized by low population and skilled densities, with implications for archaeological visibility, may also be relevant.

The case for the rest of Eurasia is more complicated. Unfortunately, Brown et al. (2012) may have over-simplified the situation when they stated that "[m]icrolith-tipped projectile weapons increased hunting success …and would have conferred substantive advantages on modern humans as they left Africa and encountered Neanderthals equipped with only hand-cast spears". Most notably, an African influence has not been demonstrated on the bladelets/microliths found in the Levant (e.g., Marks, 2003; Belfer-Cohen and Goring-Morris, 2007; Mellars et al., 2013; Hublin, 2015). In other words, the modern human dispersal out-of-Africa into the Levant likely occurred without the help of bladelets/microliths. Although bladelets have recently been reported at some IUP sites in the Levant (Boëda et al., 2015; Kadowaki, 2017) and southern Siberia (Zwyns et al., 2012), their occurrences are still limited in comparison with the later EUP assemblages, such as the Early Ahmarian. In Europe, intentional production or use of bladelets are unknown in the Bachokirian or the Bohunician (Hoffecker, 2009; Hublin, 2015). On the other hand, production of bladelets by Neanderthals is attested in several French Mousterian assemblages,

Please cite this article in press as: Wakano J.Y., et al., Ecocultural range-expansion scenarios for the replacement or assimilation of Neanderthals by modern humans. Theoretical Population Biology (2017), https://doi.org/10.1016/j.tpb.2017.09.004.

although their frequencies are lower than in Protoaurignacian assemblages (Villa and Roebroeks, 2014). In this way, we suggest that the increase in the frequency of bladelets from the IUP (and possibly the Middle Palaeolithic) to the EUP can be regarded as a potential archaeological correlate of the changing density of skilled individuals predicted by our model.

To reiterate, the replacement scenario of our model predicts a first wave of invading modern humans with low population and skilled densities, which is followed by a slower second wave with high population and skilled densities. Hence, when we focus on one region, we expect the IUP to precede the EUP, which is apparently not the case in western Europe or the Zagros/Caucasus regions. However, when the skilled density is low, any artefacts that rely on this skill for their manufacture, namely bladelets/microliths, would likely be made in quantities too small to be archaeologically visible. In addition, the model ignores the Allee effect (e.g., Roques et al., 2012) and demographic stochasticity, which if incorporated may affect our predictions where the population density is low. Thus, we submit that the empirically observed spread of the IUP and the EUP may, to a first approximation, correspond to the theoretically predicted first and second waves, respectively.

The relative sizes of Neanderthals and moderns both prior and subsequent to the expansion of the latter from Africa have been investigated using archaeological and genomic techniques. Advanced tools in Africa may have enabled expansion of numbers there prior to 70 kya (Brown et al., 2012), and analysis of mitochondrial DNA suggests that the expansion out of Africa was "prefaced by a major [demographic] expansion in Africa" (Atkinson et al., 2009). There is considerable agreement that the Neanderthal-to-modern transition was accompanied by rapid population growth (Mellars and French, 2011; Villa and Roebroeks, 2014). For these reasons we first conducted our numerical analysis assuming in Eq. (11) that the initial density $N_2(x, 0)$ in the left half of space, representing moderns in Africa, was uniformly greater than $N_1(x, 0)$ in the right half, representing Neanderthals in Eurasia.

However, the results presented here may even apply to situations in which modern humans lack an initial demographic advantage (e.g., Eq. (15)). Modern humans, who start out with a cultural advantage, will rapidly reach a demographic advantage, as shown in our previous work (Gilpin et al., 2016), if the timescale of demographic change is faster than that of cultural change (Richerson et al., 2009). When the size of the intrinsic growth rate, r, relative to the cultural transmission parameters, γ and δ, is large enough that $r > \gamma + \delta$, then any permissible $Z_2(x, 0) > Z^*$ is sufficient for invasion by the moderns as long as the other criteria for Z^* discussed above are also satisfied. However, if r is sufficiently small compared to $\gamma + \delta$, there exists a minimum value of $Z_2(x, 0)$ below which the skilled density of the moderns will decrease to that of the Neanderthals, precluding invasion. Thus $Z_2(x, 0) > Z^*$ is a necessary but not sufficient condition for moderns to invade. These and other details concerning how the initial skilled density and the key parameters r, γ, δ, affect the success of the moderns are provided in *SI* 1. It should be emphasized that the converse is also true: an initial demographic advantage does not guarantee replacement or assimilation.

Throughout our analysis, we have assumed that inequalities (1f) hold; these entail that each species in isolation can exist stably at either the high carrying capacity, M_H, or the low carrying capacity, M_L. Our main numerical results assume that initially in Eq. (2) the population sizes are given by Eqs. (11a) and (11b) in the left and right halves of the finite spatial domain. Depending on whether the competition coefficient, b, is less than or greater than M_L/M_H, either three waves (Fig. 2A) or two (Fig. 2B), respectively, form. In the former case, one monostable wave takes a small number of moderns to coexistence of both species at low densities. However, the bistable wave, in this case, continues the expansion of moderns to asymmetric coexistence, with a higher density of moderns and a lower density of archaics. This is the assimilation scenario, which is not supported by current genetic studies, as it entails that Neanderthals would have contributed to the genetic ancestry of Africans as well as Eurasians. In the latter case where competition is stronger (Fig. 2B), the bistable wave allows the moderns to completely replace the archaics, although there is a period of coexistence, which is longer near the right boundary ($x = L$) of the spatial domain. Additional numerical work shows that as b approaches 1 – i.e., when competition becomes even stronger due to further niche overlap – the duration of coexistence of the two species becomes very short (Supporting Fig. 3). It should be emphasized that assimilation or replacement may occur only when the speed of the bistable wave is positive; this places an upper bound on Z^*/θ, the ratio of the threshold skilled density to cognitive ability (or ease of acquisition of the skills) (see Eqs. (10a) and (10b); Fig. 3).

Our numerical analysis demonstrates transient periods of low coexistence between the arrivals of the monostable wave front and the bistable wave front. The duration and spatial extent of the Neanderthal-modern coexistence have been addressed in the archaeological literature. Archaeological opinions vary between "quite long on a continental scale" (Hublin, 2015) to "at most about 6000 yr …with periods of overlap within the individual regions of Europe (such as western France) of perhaps only 1000–2000 yr" (Mellars 2006) and "an overlap of minimally 2000 yr within Europe can be inferred" (Roebroeks and Soressi, 2016). In Europe, at least, there seems to be a consensus building that the overlap occurred between about 40 and 45 kya, but may not have lasted for this whole period. It may be conjectured that data from the Manot cave (Hershkovitz et al., 2015) and other as yet unexplored Middle Eastern locations, may extend the beginning of the period of overlap to 55 kya or earlier. The period of overlap inferred from archaeology provides real-world timescales for features of our model, but the qualitative properties of our model do not depend on the exact empirical values—rather, our model provides insight into the manner in which the relative magnitudes of different effects (competition, learning, etc.) contribute to different outcomes. It is comforting, however, to see that the reaction–diffusion approach does allow for coexistence in non-trivial parametric geographic and temporal ranges.

Our analyses highlight the importance of local geographic as well as temporal overlap between Neanderthals and modern humans. This overlap must have been essential for genetic introgression to occur. Our results suggest three predictions. (i) We predict that the period of local overlap, inferred either from archaeological records or from studies of (two-way) genetic introgression (Kuhlwilm et al., 2016), should be larger in regions of Europe distant from the first modern human entry site (presumably in the Levant, as in Hershkovitz et al., 2015). (ii) We predict that the strength of the dependence of local overlap period on distance from entry site (the slope of the trend lines in Fig. 4) should increase as the difficulty of the skills determining carrying capacity (as measured by θ^{-1}) increases. A very strong dependence of overlap duration on distance from the Levant would suggest that the skills were relatively difficult because the second wave must have travelled slowly relative to the first wave (Fig. 3). (iii) During the overlap of Neanderthals and modern humans, the saturation density of the latter would be lower than after Neanderthal extinction. This could appear as a decreased estimated effective population size for ancestral modern humans. Similarly, our model might be used as a baseline model for population genetic analysis such as those estimating the level of genetic exchange. The spatial extension of our earlier ecocultural analysis (Gilpin et al., 2016) focuses attention on geographical variation in both archaeological findings and degree of genetic exchange across the Levant and western Eurasia.

Please cite this article in press as: Wakano J.Y., et al., Ecocultural range-expansion scenarios for the replacement or assimilation of Neanderthals by modern humans. Theoretical Population Biology (2017), https://doi.org/10.1016/j.tpb.2017.09.004.

Acknowledgments

We thank H. Matano, K. Sano, and O. Kolodny for valuable comments. This research was supported in part by Monbukagakusho Grant 16H06412 to JYW, by the Stanford Center for Computational, Evolutionary and Human Genomics, and by the Morrison Institute for Population and Resource Studies at Stanford University.

Appendix A. Supplementary data

Supplementary material related to this article can be found online at https://doi.org/10.1016/j.tpb.2017.09.004.

References

Ammerman, A.J., Cavalli-Sforza, L.L., 1971. Measuring the rate of spread of early farming in Europe. Man 6, 674–688.
Ammerman, A.J., Cavalli-Sforza, L.L., 1973. A population model for the diffusion of early farming in Europe. In: Renfrew, C. (Ed.), The Explanation of Culture Change. Duckworth, London, pp. 343–357.
Ammerman, A.J., Cavalli-Sforza, L.L., 1984. The Neolithic Transition and the Genetics of Populations in Europe. Princeton University Press, Princeton, NJ.
Aoki, K., 1998. Modeling the spread of early farming and of the Early Upper Paleolithic in Europe. In: Omoto, K., Tobias, P. (Eds.), The Origins and Past of Modern Humans: Towards Reconciliation. World Scientific Press, Singapore, pp. 161–182.
Aoki, K., 2015. Modeling abrupt cultural regime shifts during the Palaeolithic and stone age. Theor. Popul. Biol. 100, 6–12.
Aoki, K., Lehmann, L., Feldman, M.W., 2011. Rates of cultural change and patterns of cultural accumulation in stochastic models of social transmission. Theor. Popul. Biol. 79, 192–202.
Aoki, K., Shida, M., Shigesada, N., 1996. Travelling wave solutions for the spread of farmers into a region occupied by hunter-gatherers. Theor. Popul. Biol. 50, 1–17.
Atkinson, Q.D., Gray, R.D., Drummond, A.J., 2009. Bayesian coalescent inference of major human Mitochondria DNA haplogroup expansions in africa. Proc. R. Soc. B 276, 367–373.
Banks, W.E., et al., 2008. Neandertal extinction by competitive exclusion. PLoS one 3 (12), e3972.
Banks, W.E., d'Errico, F., Zilhão, J., 2013. Revisiting the chronology of the proto-aurignacian the Early Aurignacian in Europe: a reply to higham et al.'s comments on Banks, et al. 2013. J. Hum. Evol. 65, 810–817.
Bar-Yosef, O., 2007. The archaeological framework of the Upper Paleolithic revolution. Diogenes 54, 3–18.
Bar-Yosef, O., 2013. Neanderthals and modern humans across Eurasia. In: Akazawa, T., Nishiaki, Y., Aoki, K. (Eds.), Dynamics of Learning in NeandErthals and Modern Humans Vol. 1 Cultural Perspectives. Springer, Japan, Tokyo, pp. 7–20.
Bar-Yosef, O., Belfer-Cohen, A., 2013. Following pleistocene road signs of human dispersals across Eurasia. Quat. Int. 285, 30–43.
Bar-Yosef, O., Kuhn, S.L., 1999. The big deal about blades: laminar technologies and human evolution. Am. Anthropol. 101, 322–338.
Bar-Yosef, O., Pilbeam, D., 2000. The Geography of NeandErtals and Modern Humans in Europe and the Greater Mediterranean. Peabody Museum of Archaeology and Ethnology and Harvard University, Cambridge MA.
Belfer-Cohen, A., Goring-Morris, N., 2007. From the beginning: levantine Upper Palaeolithic cultural change and continuity. In: Mellars, P., Boyle, K., Bar-Yosef, O., Stringer, C. (Eds.), Rethinking the Human Revolution: New Behavioural and Biological Perspectives on the Origin and Dispersal of Modern Humans. McDonald Institute for Archaeological Research, Cambridge, pp. 199–206.
Benazzi, S., et al., 2011. Early dispersal of modern humans in Europe and implications for neanderthal behaviour. Nature 479, 525–528.
Benazzi, S., et al., 2015. The makers of the protoaurignacian and implications for neandertal extinction. Science 348, 793–796.
Bergman, C.A., Stringer, C., 1989. Fifty years after: Egbert, and early Upper Palaeolithic juvenile from Ksar Akil, Lebanon. Paléorient 15, 99–111.
Boëda, E., et al., 2015. Un débitage lamellaire au proche-orient vers 40,000 ans cal BP le site d'umm el tlel, Syrie Centrale. L'Anthropologi 119, 141–169.
Brown, K.S., et al., 2012. An early and enduring advance technology originating 71,000 years ago in south africa. Nature 491 (7425), 590–593.
Caldwell, C.A., Millen, A.E., 2010. Human cumulative culture in the laboratory: effects of (micro) population size. Learn. Behav. 38, 310–318.
Cavalli Sforza, L.L., Feldman, M.W., 1981. Cultural Transmission and Evolution: A Quantitative Approach. Princeton University Press, Princeton N.J.
Clark, J.L., 2011. The evolution of human culture during the later pleistocene: Using fauna to test models on the emergence and nature of "modern" human behavior. J. Anthropol. Archaeol. 30, 273–291.
Collard, M., Vaesen, K., Cosgrove, R., Roebroeks, W., 2016. The empirical case against the 'demographic turn' in palaeolithic archaeology. Philos. Trans. R. Soc. Lond. B Biol. Sci. 371, 20150242.
Currat, M., Excoffier, L., 2004. Modern humans did not admix with Neanderthals during their range expansion into Europe. PLoS Biol. 2 (12), e421.
Currat, M., Excoffier, L., 2011. Strong reproductive isolation between humans and Neanderthals inferred from observed patterns of introgression. Proc. Natl. Acad. Sci. USA 108, 15129–15134.
Currat, M., Ruedi, M., Petit, R.J., Excoffier, L., 2008. The hidden side of invasions: Massive introgression by local genes. Evolution 62, 1908–1920.
Derex, M., Beugin, M.P., Godelle, B., Raymond, M., 2013. Experimental evidence for the influence of group size on cultural complexity. Nature 503, 389–391.
Eren, M.I., Greenspan, A., Sampson, C.G., 2008. Are upper paleolithic blade cores more productive than middle paleolithic discoidal cores? A replication experiment. J. Hum. Evol. 55, 952–961.
Fisher, R.A., 1937. The wave of advance of advantageous genes. Ann. Eugenics 7, 355–369.
Flores, J.C., 1998. A mathematical model for Neanderthal extinction. J. Theoret. Biol. 191, 295–298.
Flores, J.C., 2011. Diffusion coefficient of modern humans outcompeting Neanderthals. J. Theoret. Biol. 280, 189–190.
Fogarty, L., Wakano, J.Y., Feldman, M.W., Aoki, K., 2015. Factors limiting the number of independent cultural traits that can be maintained in a population. In: Mesoudi, A., Aoki, K. (Eds.), Learning Strategies and Cultural Evolution During the Palaeolithic. Springer, Tokyo, pp. 9–21.
Fogarty, L., Wakano, J.Y., Feldman, M.W., Aoki, K., 2017. The driving forces of cultural complexity: Neanderthals, modern humans, and the question of population size. Hum. Nat. (in press).
Fort, J., Pujol, T., Cavalli-Sforza, L.L., 2004. Palaeolithic populations and waves of advance. Camb. Archaeol. J. 14, 53–61.
Fu, Q., et al., 2014. Genome sequence of a 45,000-year-old modern human from western Siberia. Nature 514, 445–450.
Ghirlanda, S., Enquist, M., 2007. Cumulative culture and explosive demographic transitions. Qual. Quant. 41, 591–600.
Gilpin, W., Feldman, M.W., Aoki, K., 2016. An ecocultural model predicts Neanderthal extinction through competition with modern humans. Proc. Natl. Acad. Sci. USA 113, 2134–2139.
Green, R.E., et al., 2010. A draft sequence of the Neandertal genome. Science 328, 710–722.
Henrich, J., 2004. Demography and cultural evolution: how adaptive cultural processes can produce maladaptive losses—the tasmanian case. Am. Antiq. 69, 197–214.
Hershkovitz, I., et al., 2015. Levantine cranium from manot cave (Israel) foreshadows the first European humans. Nature 520, 216–219.
Higham, T., et al., 2014. The timing and spatiotemporal patterning of Neanderthal disappearance. Nature 512, 306–309.
Hiscock, P., Clarkson, C., MacKay, A., 2011. Big debates over little tools: ongoing disputes over microliths on three continents. World Archaeol. 43, 653–664.
Hoffecker, J.F., 2009. The spread of modern humans in Europe. Proc. Natl. Acad. Sci. USA 106, 16040–16045.
Horan, R.D., Bulte, E.H., Shogren, J.F., 2005. How trade saved humanity from biological exclusion: the Neanderthal enigma revisited and revised. J. Econ. Behav. Organ. 58, 1–29.
Hosono, Y., 1998. The minimal speed of traveling fronts for a diffusive Lotka–Volterra competition model: dedicated to the memory of Akira Okubo. Bull. Math. Biol. 60, 435–438.
Hublin, J.-J., 2015. The modern human colonization of western Eurasia: when and where? Quat. Sci. Rev. 118, 194–210.
Hublin, J.-J., Roebroeks, W., 2009. Ebb and flow or regional extinctions? On the character of Neandertal occupation of northern environments. C. R. Palevol. 8, 503–509.
Kadowaki, S., 2013. Issues of chronological and geographical distributions of middle and upper palaeolithic cultural variability in the levant and implications for the learning behavior of Neanderthals and Homo Sapiens. In: Akazawa, T., Nishiaki, Y., Aoki, K. (Eds.), Dynamics of Learning in NeandErthals and Modern Humans Volume 1 Cultural Perspectives. Springer, Tokyo, pp. 59–91.
Kadowaki, S., 2017. Technology of striking platform preparation on lithic debitage from Wadi Aghar, Southern Jordan, and its relevance to the initial Upper Palaeolithic technology in the levant. Al-Rāfidān 38, 23–32.
Kadowaki, S., Omori, T., Nishiaki, Y., 2015. Variability in early ahmarian lithic technology and its implications for the model of levantine origin of the protoaurignacian. J. Hum. Evol. 82, 67–87.
Klein, R.G., 2008. Out of Africa and the evolution of human behavior. Evol. Anthropol. 17, 267–281.
Klein, R.G., Steele, T.E., 2013. Archaeological shellfish size and later human evolution in Africa. Proc. Natl. Acad. Sci. USA 110, 10910–10915.
Kline, M.A., Boyd, R., 2010. Population size predicts technological complexity in Oceania. Proc. R. Soc. Lond. B Biol. Sci. 277, 2559–2564.
Kobayashi, Y., Aoki, K., 2012. Innovativeness, population size and cumulative cultural evolution. Theor. Popul. Biol. 82, 38–47.
Kolmogoroff, A., Petrovsky, I., Piscounoff, N., 1937. Étude de l'équation de la diffusion avec croisssance de la quantité de matière et son application a un problème biologique. Bull. Univ. D'état. Moscou Ser. Internat. Sect. A 1, 1–25.

Kuhlwilm, M., et al., 2016. Ancient gene flow from early modern humans into estern Neanderthals. Nature 530, 429–433.
Kuhn, S.L., 2002. Pioneers of microlithization: the proto-aurignacian of southern Europe. In: Elston, R.G., Kuhn, S.L. (Eds.), Thinking Small: Global Perspectives on Microlithization. pp. 83–93 (Archaeological Papers of the American Anthropological Association12).
Kuhn, S.L., et al., 2009. The Early Upper Paleolithic occupations at ÜçağızlıCave (Hatay, Turkey). J. Hum. Evol. 56, 87–113.
Kuhn, S.L., Zwyns, N., 2014. Rethinking the Initial Upper Paleolithic. Quat. Int. 347, 29–38.
Lee, R.D., 1986. Malthus and boserup: A dynamic synthesis. In: Coleman, D., Schofield, R. (Eds.), The State of Population Theory. Basil Blackwell, Oxford, pp. 96–130.
Lehmann, L., Aoki, K., Feldman, M.W., 2011. On the number of independent cultural traits carried by individuals and populations. Philos. Trans. R. Soc. Lond. B Biol. Sci. 366, 424–435.
Marks, A., 2003. Reflections on levantine upper palaeolithic studies: past and present. In: Goring Morris, A.N., Belfer-Cohen, A. (Eds.), More than Meets the Eye: Studies on Upper Palaeolithic Diversity in the Near East. Oxbow Books, Oxford, pp. 249–264.
Mellars, P., 2006a. A new radiocarbon revolution and the dispersal of modern humans into Eurasia. Nature 439, 931–935.
Mellars, P., 2006b. Going east: new genetic and archaeological perspectives on the modern human colonization of Eurasia. Science 313, 796–800.
Mellars, P., 2006c. Why did modern human populations disperse from Africa ca. 60,000 years ago? A new model. Proc. Natl. Acad. Sci. USA 103, 9381–9386.
Mellars, P., French, J.C., 2011. Tenfold population increase in western Europe at the Neandertal-to-modern human transition. Science 333, 623–627.
Mellars, P., et al., 2013. Genetic and Archaeological perspectives on the initial modern human colonization of Southern Asia. Proc. Natl. Acad. Sci. USA 110, 10699–10704.
Mesoudi, A., 2011. Variable cultural acquisition costs constrain cumulative cultural evolution. PLoS one 6 (3), e18239.
Muthukrishna, M., Shulman, B.W., Vasilescu, V., Henrich, J., 2014. Sociality influences cultural complexity. Proc. R. Soc. Lond. B Biol. Sci. 281, 20132511.
Nigst, P.R., et al., 2014. Early modern human settlement of Europe north of the Alps occurred 43,500 years ago in a cold steppe-type environment. Proc. Natl. Acad. Sci. USA 111, 14394–14399.
Petraglia, M., et al., 2007. Middle Paleolithic assemblages from the indian subcontinent before and after the toba super-eruption. Science 317, 114–116.
Powell, A., Shennan, S., Thomas, M.G., 2009. Late Pleistocene demography and the appearance of modern human behavior. Science 324 (5932), 1298–1301.
Prüfer, K., et al., 2014. The complete genome sequence of a Neanderthal from the altai mountains. Nature 505, 43–49.
Read, D., 2006. Tasmanian knowledge and skill: maladaptive imitation or adequate technology. Am. Antiq. 71, 164–184.
Reich, D., et al., 2010. Genetic history of an archaic hominin group from denisova cave in Siberia. Nature 468, 1053–1060.
Richerson, P.J., Boyd, R., Bettinger, R.L., 2009. Cultural innovations and demographic change. Hum. Biol. 81, 211–235.
Richter, J., 2016. Leave at the height of the party: a critical review of the Middle Paleolithic in Western Central Europe from its beginnings to its rapid decline. Quat. Int. 411, 107–128.
Roebroeks, W., Soressi, M., 2016. Neandertals revised. Proc. Natl. Acad. Sci. USA 113, 6372–6379.
Roques, L., Garnier, J., Hamel, F., Klein, E.K., 2012. Allee effect promotes diversity in traveling waves of colonization. Proc. Natl. Acad. Sci. USA 109, 8828–8833.
Roussel, M., Soressi, M., Hublin, J.-J., 2016. The Châtelperronian conundrum: blade and bladelet lithic technologies from quinçay, France. J. Hum. Evol. 95, 13–32.
Shennan, S., 2001. Demography and cultural innovation: a model and its implications for the emergence of modern human culture. Camb. Archaeol. J. 11, 5–16.
Shigesada, N., Kawasaki, K., 1997. Biological Invasions: Theory and Practice. Oxford Univ. Press, Oxford.
Škrdra, P., 2003. Comparison of Boker Tachtit and Stránská skála MP/UP transitional industries. J. Israel Prehist Soc. 33, 37–73.
Strimling, P., Sjöstrand, J., Enquist, M., Eriksson, K., 2009. Accumulation of independent cultural traits. Theor. Popul. Biol. 76, 77–83.
Stringer, C.C., Barton, R.N.E., Finlayson, J.C. (Eds.), 2000. NeandErthals on the Edge: 10th Anniversary Conference of the Forber'S Quarry Discovery, Gibraltar. Oxbow Books, Oxford.
Vaesen, K., Collard, M., Cosgrove, R., Roebroeks, W., 2016. Reply to Henrich et al: The Tasmanian effect and other red herrings. Proc. Natl. Acad. Sci. USA 113 (44), E6726–E6727.
Villa, P., Roebroeks, W., 2014. Neanderthal demise: an Archaeological analysis of the modern human superiority complex. PLoS one 9 (4), e96424.
Wakano, J.Y., 2006. A mathematical analysis of public goods games in the continuous space. Math. Biosci. 201, 72–89.
Wakano, J.Y., Kawasaki, K., Shigesada, N., Aoki, K., 2011. Coexistence of individual and social learners during range expansion. Theor. Popul. Biol. 80, 132–140.
Wang, M.-X., Lai, P.-Y., 2012. Population dynamics and wave propagation in a Lotka–Volterra system with wave propagation. Phys. Rev. E 86, 051908.
Welker, F., et al., 2016. Palaeoproteomic evidence identifies archaic hominins associated with the Châtelperronian at the grotte du renne. Proc. Natl. Acad. Sci. USA 113 (40), 11162–11167.
Wynn, T., Overmann, K.A., Coolidge, F.L., 2016. The false dichotomy: a refutation of the Neandertal indistinguishability claim. J. Anthropol. Sci. 94, 1–22.
Zilhão, J., 2007. The emergence of ornaments and art: an archaeological perspective on the origins of "behavioral modernity". J. Archaeol. Res. 15, 1–54.
Zilhão, J., et al., 2010. Symbolic use of marine shells and mineral pigments by Iberian Neandertals. Proc. Natl. Acad. Sci. USA 107, 1023–1028.
Zwyns, N., et al., 2012. Burin-core technology and laminar reduction sequences in the Initial Upper Paleolithic from Kara-Bom (Gorny-Altai, Siberia). Quat. Int. 259, 33–47.

Please cite this article in press as: Wakano J.Y., et al., Ecocultural range-expansion scenarios for the replacement or assimilation of Neanderthals by modern humans. Theoretical Population Biology (2017), https://doi.org/10.1016/j.tpb.2017.09.004.